Ground Fault Protection for Resistance-Grounded Collector Feeders With Inverter-Based Resources

Ryan McDaniel and Ritwik Chowdhury
Schweitzer Engineering Laboratories, Inc.

Presented at the
49th Annual Western Protective Relay Conference
Spokane, Washington
October 11–13, 2022

Ground Fault Protection for Resistance-Grounded Collector Feeders With Inverter-Based Resources

Ryan McDaniel and Ritwik Chowdhury, *Schweitzer Engineering Laboratories, Inc.*

***Abstract*—Ground fault protection for medium-voltage (MV) collector feeders that connect to dispersed inverter-based resources (IBRs), such as wind farms, can be provided by nondirectional overcurrent (51G), directional overcurrent (67G), and distance elements (21G).**

The 21G and 67G elements in use today have been fine-tuned for optimal performance in effectively grounded systems and can face challenges in resistance-grounded MV collector feeders, where ground fault currents can be capacitive. IBRs may inject negative-sequence current (3I2) that is incoherent with the negative-sequence voltage during a fault. Therefore, to maintain adequate security for reverse faults, a negative-sequence directional (32Q) element needs to be desensitized. At the same time, resistance grounding limits 3I2 from the grid during ground faults. The result is that the 32Q element may not be dependable for single-line-to-ground faults. This paper discusses the use of a zero-sequence directional element (32V) that is tuned to the capacitive resistance-grounded system for improved directionality.

Dynamic mho elements that use positive-sequence memory polarization contract and expand to provide enhanced security and dependability in inductive systems. In resistance-grounded capacitive systems, their reliability is reduced. Quadrilateral elements face similar polarization challenges. This paper discusses the use of nondirectional offset distance characteristics to improve the distance element performance in these systems.

Security and dependability improvements for other ancillary logic are discussed. Use of voltage-based fault-type identification improves selection of the appropriate ground distance loop. Use of timers that can ride through the dropout of intermittent faults improves dependability of time-delayed protection schemes. The solutions provided in this paper have been validated using field data and real-time digital simulator testing.

I. Introduction

Ground fault protection using the ground distance (21G) element provides improved selectivity over directional ground overcurrent protection (67G) by providing a controllable reach that does not vary in systems where the fault current changes based on available generation. The 21G element is commonly applied to detect single line-to-ground (LG) faults in high-voltage transmission lines. It can trip high-speed for faults within an underreaching Zone 1. The 21G element can also be applied as an overreaching Zone 2 as part of a pilot scheme to trip for faults throughout the protected line or with time-delays to provide backup protection for faults beyond the remote line terminal.

In a high-voltage transmission system, a 67G element's lack of selectivity preclude using it as a Zone 1 element, but it can be used in a pilot scheme to provide additional sensitivity for high-resistance faults that the 21G element may not detect. Directional ground-time overcurrent (51G) and/or negative-sequence time-overcurrent (51Q) can provide sensitive and time-delayed backup to the 67G and 21G elements.

The 21G elements in use today have been fine-tuned for optimal performance in effectively grounded systems with conventional generation. They rely on the following traditional system characteristics:

1. The currents and voltages have the same frequency and remain coherent with each other. The frequency does not change significantly during a fault.
2. The negative-sequence and zero-sequence source impedances are assumed to be passive and linear and do not change significantly during a fault.
3. The system impedances in the positive-, negative-, and zero-sequence networks are overall inductive.

The 21G elements, both the mho and quadrilateral characteristics, commonly use positive-sequence memory voltage ($V1_{MEM}$). The 21G mho element uses $V1_{MEM}$ to define the circle characteristic, whereas the 21G quadrilateral can use $V1_{MEM}$ to define the directional line. Using $V1_{MEM}$ provides benefits in traditional systems such as increased fault-resistance coverage, security during a single-phase open, favorable adaptability during load-flow, and reliability for zero-voltage ground faults [1]. While these features are desirable, the associated cost is that these elements are reliable only in systems where all three characteristics are met. The 21G element is also often supervised by fault-type identification and selection (FIDS) logic, which relies on traditional system characteristic 2 [2].

The 21G and 67G elements are supervised by directional elements. The directional element may compare the negative-sequence voltage (3V2) and negative-sequence current (3I2). It may also compare the zero-sequence voltage (3V0) and zero-sequence current (3I0). In systems with inverter-based resources (IBRs), the 32Q element may require desensitization to avoid a misoperation resultant from the lack of coherence between 3V2 and 3I2 [2]. The issue occurs because of a difference in frequency of the 3I2 injected by the IBR compared to the 3V2 because of the active control response of the IBR, which violates traditional system characteristics 1 and 2.

The 32V element can be used for reliable ground fault directionality in IBR systems because the wind turbine generators (WTGs) or solar photovoltaic (PV) generation sources are isolated in the zero-sequence network. This means that the zero-sequence network is passive and protection elements that use 3I0 can continue to be set sensitively [3]. However, the use of the 32V element in resistance-grounded systems can violate traditional system characteristic 3 because

the zero-sequence network may be capacitive rather than inductive [4] [5].

More systems at all voltage levels violate traditional system characteristics 1 and 2 with the proliferation of IBRs. At transmission voltage levels, standardized responses from IBRs are expected to help, but the control response of an IBR is not standardized within the first few cycles when transmission line primary protection is expected to operate [6]. Transmission line protection elements are seeing widespread applications at lower voltage levels because they are often not cost-prohibitive. However, as noted earlier, medium-voltage (MV) resistance grounding is more common than in the high-voltage (HV) transmission system and can violate traditional system characteristic 3 [7]. Increased penetration of IBRs combined with the increased use of transmission line protection elements at the MV level requires new solutions for reliability.

In this paper, we discuss challenges and solutions to applying 21G and 67G elements in the non-traditional application of MV collector feeder protection at an IBR plant. Section II details the challenges in applying 21G/67G protection in a resistance-grounded system. Section III discusses additional challenges caused by the presence of IBRs. Section IV provides solutions to the protection challenges in these systems.

II. Challenges to Traditional Protection Elements in Resistance-Grounded Systems

For the following discussion, we refer to Fig. 1, which illustrates a resistance-grounded IBR plant. The collector feeders, numbered 1 through N, are underground cables that connect the wind turbines to the MV collector bus. The IBR plant transformer MV winding uses a neutral grounding resistor (NGR) to limit the fault current for LG faults in the collector system. Because the LG fault current is limited by the NGR, the distributed cable capacitance to ground can be a significant portion of the fault current and requires consideration [4] [5].

The zones of protection for the collector feeder, as defined from the relaying point denoted with a flag, are shown in Fig. 1. If the cable impedance between the collector bus and the first WTG is large enough, a Zone 1 can be used for fast and selective tripping. A Zone 2 can be set to reach into, but not past, the WTG step-up transformers (WTGSUs) to provide protection for the entire feeder. Zone 2 coordinates with the MV fuses of the WTGSU (or similar protection) to maintain selectivity and avoid an outage of the entire collector feeder for a fault on the WTGSU delta winding.

To focus on the effects of the NGR and MV network cable capacitances, we simulated the system of Fig. 1 and placed collector feeder faults with an open-circuit on the WTGSU low-voltage (LV) wye winding. The behavior of the IBRs varies by type, vendor, and firmware [2], so we elected not to simulate them. We address worst-case scenarios for IBR performance in the solutions section of this paper. The collector feeder relay was set based on the impedance to the first WTGSU with Zone 1 set to 80 percent and Zone 2 set to 150 percent.

Fig. 2 shows the zero-sequence network for an AG fault on Feeder 1 of Fig. 1 to aid in explaining the behavior of the traditional 32Q, 32V, and 21G elements. In this paper, traditional elements refer to elements that are optimized for use in a traditional system that meet traditional system characteristics 1 through 3. This includes, but is not limited to, 21G elements that are inherently directional from the use of positive-sequence memory polarization.

To help quantify the capacitive reactance, we assume that each feeder has equal length and that the total capacitive reactance (XC0) of all the feeders in parallel is 1 per unit. This makes the capacitance of a single faulted feeder equal to N per unit, and the remaining unfaulted feeders as N/(N–1) per unit. The NGR is sized to limit the fault current levels per [8]. The location of the fault on the collector feeder is given in per unit from the relay location as *m*.

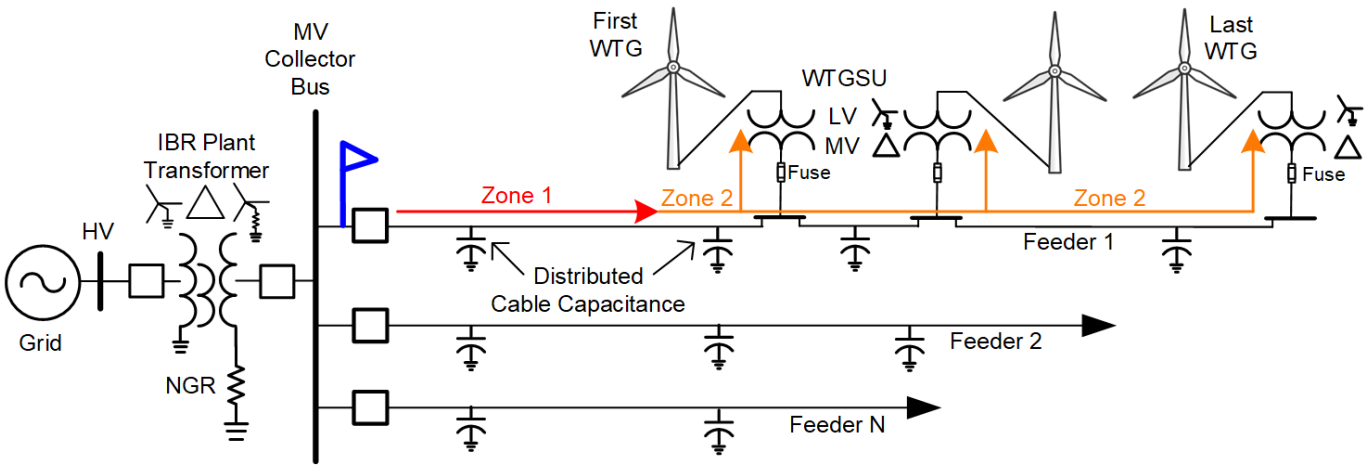

Fig. 1. Zones of protection on a resistance-grounded wind-farm collector feeder

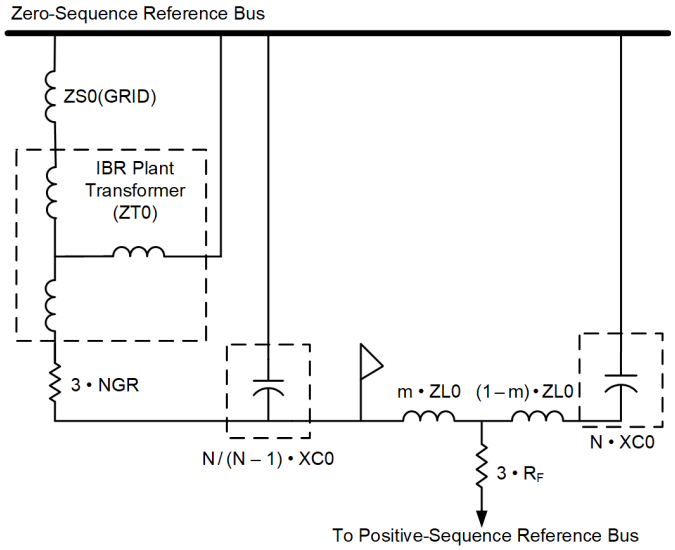

Fig. 2. Zero-sequence network for a forward ground fault

A. *Forward Faults*

First, we analyze protection element performance for a metallic LG fault at the MV terminal of the first WTGSU on the protected feeder. For this fault, the relay measures 3I0 from the NGR in parallel with the unfaulted collector feeder capacitance, i.e., N/(N–1) • XC0 from Fig. 2.

1) $V1_{MEM}$ Polarized Mho Characteristic

Fig. 3 shows the characteristic shape of the Zone 1 and Zone 2 memory-polarized mho elements.

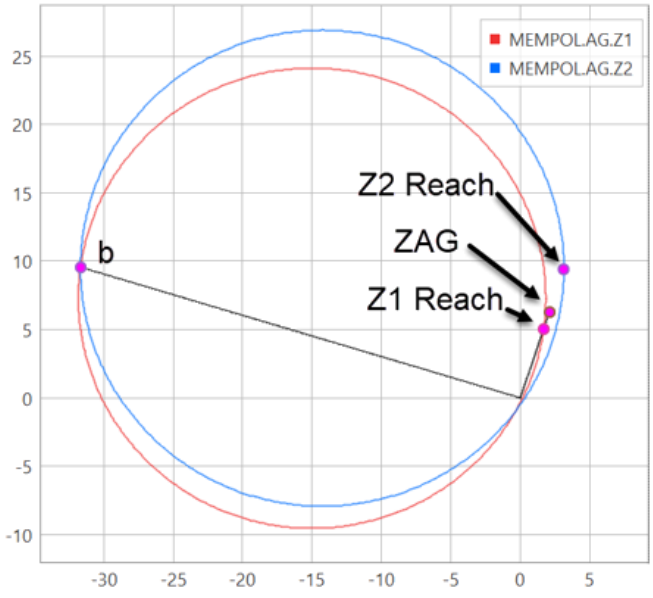

Fig. 3. Memory-polarized Zone 1 and Zone 2 mho characteristics

Point *b* is the location of the dynamic reach point of the $V1_{MEM}$ polarized mho element for a forward fault and is defined by (1) [9].

$$b_{Forward} = -\left[\frac{V1_{MEM} - VA}{I_{AG}}\right] = -ZS1_{APP} \tag{1}$$

Where I_{AG} of the line is defined by (2) and the line zero-sequence compensation factor ($k0_L$) is defined by (3). The value of k_{0L} may be challenging to determine accurately for HV ac cables [10].

$$I_{AG} = I_A + k0_L \bullet I_G \tag{2}$$

$$k0_L = \left[\frac{ZL0 - ZL1}{3 \bullet ZL1}\right] \tag{3}$$

The other known point on the circle is the reach setting, which is fixed and does not change during the fault.

To better understand point *b*, a fault-loop polarized mho, also referred to as a self-polarized mho, uses the loop voltage (VA) in place of $V1_{MEM}$ in (1). For this type of polarization, *b* evaluates to 0 and this keeps the circle static in apparent impedance plane. The self-polarized mho is not reliable for close-in faults [1].

By using $V1_{MEM}$ for polarization, point *b* will be equal to the negative of the apparent positive-sequence source impedance ($-ZS1_{APP}$) for faults on an unloaded system. This is because the numerator of (1) is the voltage drop across ZS1 and the denominator of (1) is the current through ZS1. In an inductive system, this places point *b* in quadrant 3 of the apparent impedance plane and provides dependability for close-in faults and greater fault-resistance coverage compared to the self-polarized mho element.

In our test system, the reactive portion of $ZS1_{APP}$ appears more resistive and capacitive than inductive because point *b* is in quadrant 2. The reason $ZS1_{APP}$ does not agree with the actual ZS1 is because the k0 factor of the source, $k0_S$, is very different from $k0_L$ defined in (3). Because NGR >> ZT0, we ignore ZT0 and ZS0 to simplify $k0_S$, as shown in (4).

$$k0_s = \left[\frac{3 \bullet NGR \,||\left(\frac{N}{N-1} \bullet XC0\right) - ZS1}{3 \bullet ZS1}\right] \tag{4}$$

The parallel combination of the NGR and the cable capacitances (XC0) behind the relaying point are significantly larger than the positive-sequence impedance behind the relay, making $k0_S$ quite different from $k0_L$.

To correctly measure the source impedance and provide the proper dynamic expansion for the system, I_{AG} would need be calculated with (4) rather than (3). However, if that was done, the apparent impedance to the fault (ZAG) would be incorrectly measured. The apparent ZS1 seen by the relay is shown in (5) with the derivation shown in Appendix A.

$$ZS1_{APP} = ZS1 \bullet \left[\frac{1 + k0_S}{1 + k0_L}\right] \tag{5}$$

Because of the mismatch between $k0_S$ and $k0_L$, point *b* is pushed into quadrant 2 since $k0_L$ does not account for the NGR or cable capacitance behind the relaying point. This reduces the resistive coverage of the mho element. Fig. 4 is a zoomed-in version of Fig. 3 that shows the apparent impedance (ZAG) compared to the effective dynamic mho characteristic. It clearly shows the limited resistive reach of the $V1_{MEM}$ polarized mho element. ZAG is plotted at the location of the first WTG, which is correctly measured using $k0_L$.

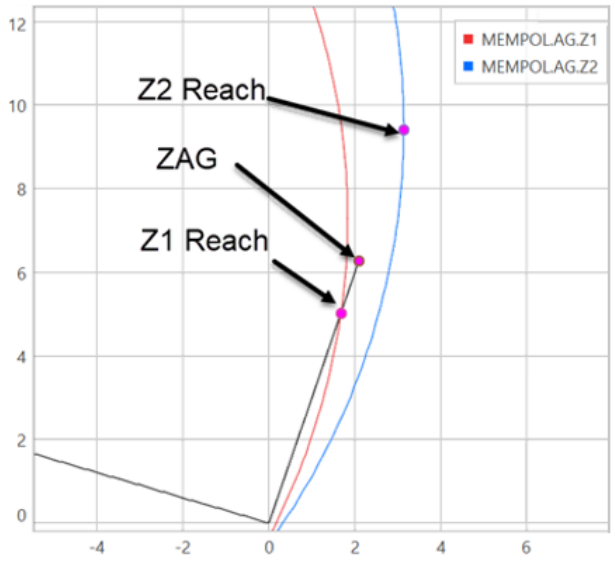

Fig. 4. Memory-polarized mho zones of Fig. 3 zoomed in

The N/(N–1) • XC0 term in (4) decreases as the number of unfaulted collector feeders (N) increase. This moves point *b* up, further reducing resistive coverage of the mho element and possibly leading to a complete loss of dependability for close-in faults.

2) $V1_{MEM}$ Polarized Quadrilateral Characteristic Directional Line

The quadrilateral element is typically supervised by a directional element that uses $V1_{MEM}$ and is implemented using (6) [1]. Z1ANG is the positive-sequence line impedance angle.

$$\mathrm{RE}[V1_{MEM} \bullet (IAG \bullet 1\angle Z1ANG)^*] > 0 \qquad (6)$$

We can evaluate the location of the directional line in the ZAG plane by recognizing that this is similar to an impedance line set with a reach of zero ohms, and by defining an operate (SOP) and polarizing (SPOL) quantity (7). The method used in [11] can then be used to plot the characteristic.

$$\begin{aligned} SOP &= V1_{MEM} - IAG \bullet 0 \\ SPOL &= IAG \bullet (1\angle Z1ANG) \end{aligned} \qquad (7)$$

Appendix B shows that the forward reach effectively becomes $(-ZS1_{APP})$ and reverse reach becomes $-\infty \angle Z1ANG$. This describes a line that is perpendicular to Z1ANG and intersects $-ZS1_{APP}$. The directional line from the fault located at the first WTG is shown in Fig. 5.

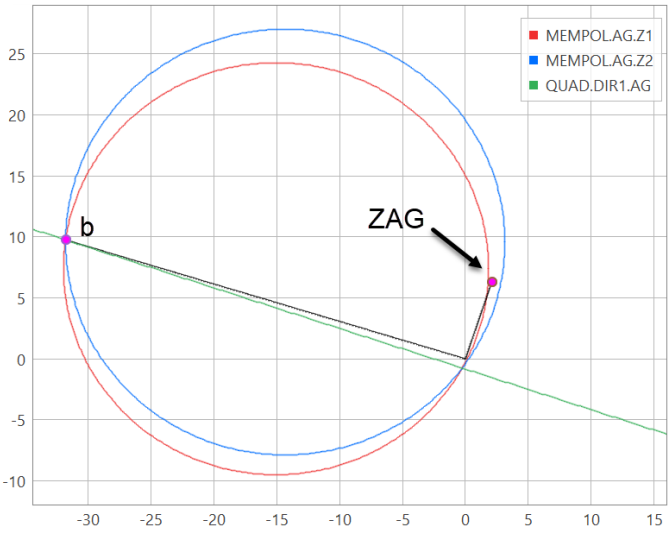

Fig. 5. Quadrilateral directional line added to mho zones of Fig. 3

If ang(b) – Z1ANG is less than 90 degrees, the directional line shifts above the origin and the relay loses dependability for close-in faults. This can happen as N in Fig. 2 increases and pushes point *b* up in the second quadrant, which pushes the directional line up the Z1ANG line so it does not encompass the origin. This can also degrade the dynamic mho element dependability as a directional line often supervises these elements [1].

3) Zero-Sequence Directional Element

The characteristic plot of the zero-sequence impedance directional element is shown in Fig. 6. This element takes the apparent zero-sequence impedance seen by the relay and compares it to settable thresholds [12] [13].

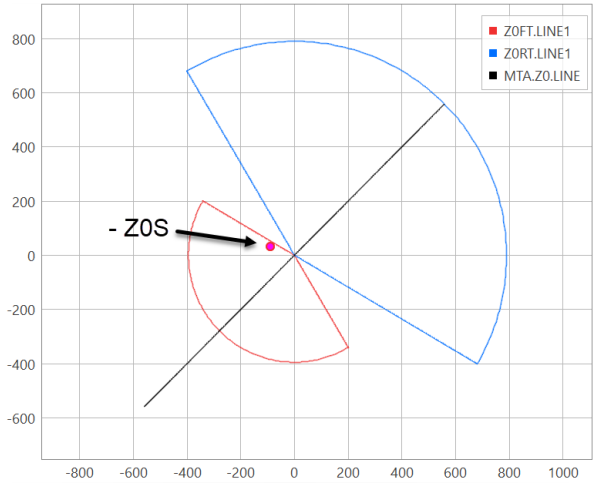

Fig. 6. Zero-sequence directional element (32V) characteristics

The red characteristic is the forward directional line with an impedance threshold set to –0.3 ohms secondary and a circular boundary with a radius equal to the magnitude of the measured V0 divided by the overcurrent pickup setting of the forward element. The lower the overcurrent pickup is set, the larger the radius of the circle. The blue characteristic is similarly defined, but with an impedance threshold setting of +0.3 ohms secondary and a circular boundary with a radius of the measured V0 divided by the overcurrent pickup setting for the

reverse element. The reverse current pickup setting is smaller than the forward making the reverse characteristic larger in the Z0 plane. The maximum torque angle (MTA) setting is set to 45 degrees, which is the zero-sequence impedance angle of the feeder. The Z0 measured by the relay, which is negative of the zero-sequence impedance of the source (–Z0S), does fall within the forward characteristic, but far from the MTA of the element. As N in Fig. 2 becomes larger, –Z0S moves up in the second quadrant of the Z0 plane and outside the forward operating region.

B. Reverse Fault

Next, we look at the performance of the different elements for an LG fault on an adjacent feeder. For this fault, the only source of current for the relay is the zero-sequence capacitive reactance of a single unfaulted feeder because the IBR is disconnected.

1) $V1_{MEM}$ Polarized Mho Characteristic and Quadrilateral Characteristic Directional Line

Point *b* for a reverse fault is primarily defined by the zero-sequence capacitive reactance of the feeder and plots in quadrant 4. Fig. 7 shows the entire characteristic. For this reverse fault, the capacitive reactance of the line creates an expansion of the mho characteristic, rather than contraction, and leads to a security concern. Appendix C shows that the approximate location of point *b* is (8) when the IBR is disconnected.

$$b_{Reverse} = -Z0R \bullet \left[\frac{Z1L}{Z0L}\right] \tag{8}$$

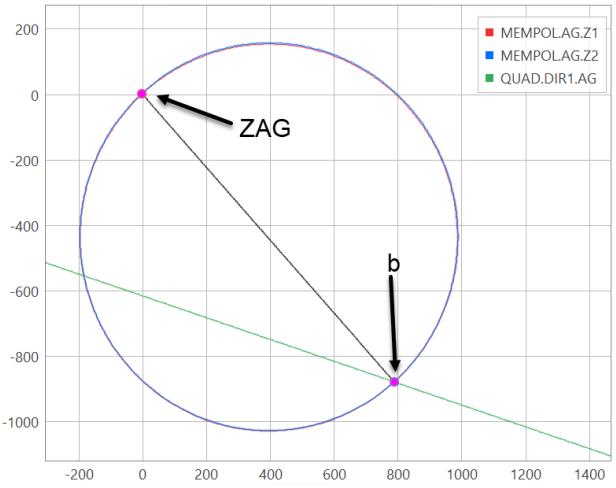

Fig. 7. Mho and quad directional line for reverse fault

Fig. 8 is zoomed in to show where ZAG plots relative to the distance characteristics.

Assuming the 21G supervisory checks associated with fault-loop selection and overcurrent are satisfied, the Zone 2 mho element would operate, and the quadrilateral directional line would declare forward.

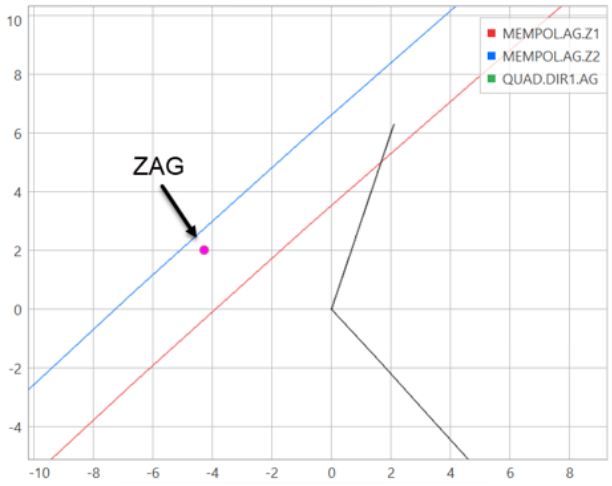

Fig. 8. Mho and quad directional line for a resistive fault zoomed in

The ZAG impedance is not in the traditional reverse direction (quadrant 3). This is because of the infeed effect where the apparent impedance measured by the relay is mostly affected by the NGR and adjacent collector feeder contribution rather than the small capacitive contribution from the collector feeder the relay is protecting. Reference [14] includes discussion on infeed effect as it relates to forward-reaching elements, but the same discussion applies to reverse-looking elements.

2) The Zero-Sequence Directional Element

The zero-sequence directional element characteristic is shown in Fig. 9.

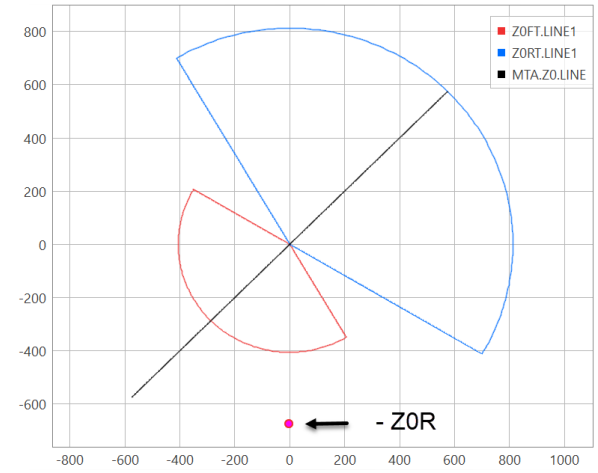

Fig. 9. Zero-sequence directional element for a reverse fault

The element does not declare forward because the associated overcurrent supervision is set above the capacitive current contribution of a single feeder. However, the apparent zero-sequence impedance measured by the relay for this reverse fault is in a traditional system's forward direction. A reverse fault in a capacitive system looks like a forward fault in an inductive system.

C. *Intermittent Arcing Faults*

Ground faults on the resistance-grounded MV collector feeder cable network are often intermittent in nature. Reference [7] presents field events of these arcing ground faults in wind farms. These intermittent faults do not produce a stable apparent impedance measurement, which can challenge dependability of time-delayed protection elements.

III. Additional Challenges in Systems With IBRs

IBRs have little to no physical inertia compared to conventional generators. The considerations for transmission line protection near IBRs, as detailed in [2], are also applicable to the collector system using distance protection. Reference [2] shows that for an unbalanced fault, 3I2 may not be coherent with 3V2 and can have a different frequency because of the IBR control response. This leads to recommendations of increasing the 32Q overcurrent supervision settings based on the IBR ratings and relying on the 32V element for ground faults [3]. Current-based FIDS that uses the phase relationship between 3I2 and 3I0 is also unreliable. The solution to mitigate these issues is to use voltage-based FIDS [14] [3]. Because the IBR is a weak source, the faulted phase voltages collapse and can be used to identify the faulted loop. By using voltage to detect the faulted loops, reliance on 3I2 is reduced.

In the MV collector system with an NGR, the faulted phase voltage collapses for LG faults, even if the grid is strong. Therefore, the same recommendations for transmission line protection given in [3] can be applied to the collector feeder as well—by increasing the 3I2 overcurrent supervision for the directional element and current-based FIDS above the collector feeder IBR megavolt ampere (MVA) rating (not the total IBR plant rating). This prevents the 32Q element from providing directionality for LG faults on the collector feeder, deferring the directionality to the 32V element instead. This helps the relay remain secure for reverse faults.

For line-to-line-to-ground (LLG) faults on the feeder, the phase distance element (21P) is expected to clear the fault. If the grid is strong, the traditional 21P element is dependable. If the grid is weak, there may be reduced dependability from the 21P element if it uses 32Q supervision because of the possible incoherent relationship between 3I2 and 3V2. However, the 3I2 magnitude, as contributed from the weak grid and the N/(N–1) IBRs, can still exceed the secure overcurrent supervision set based on a single collector feeder's rating. Therefore, instead of relying on a traditional 21P element supervised by a 32Q element, another 21P element supervised by a securely set nondirectional 50Q element can be used to improve LLG fault dependability in weak systems. In short, the relay can be set such that if the grid is strong, traditional 21P is enabled for LLG faults. If the grid is weak, a different set of 21P elements better suited for use near IBRs can be enabled.

IV. Solutions

A. *21G Using Fault-Loop Polarization (Self-Polarization)*

To prevent security and dependability issues associated with the use of $V1_{MEM}$ polarization, we use fault-loop polarized elements. Fault-loop polarized distance elements remain static in the impedance plane, which makes their behavior predictable in challenging systems. Because these elements may not be dependable for close-in faults, a reverse reach setting is used to add dependability. Having a reverse reach also makes these elements nondirectional, so they require appropriate directional supervision. Fig. 10 shows the offset characteristic as well as the apparent impedance for a Zone 2 fault (Section II. A) and a reverse fault (Section II. B). The mho and quadrilateral characteristics are discussed in detail in [14] and implemented in [15] with relay logic. These elements can be used in addition to the traditional distance elements available in the relay.

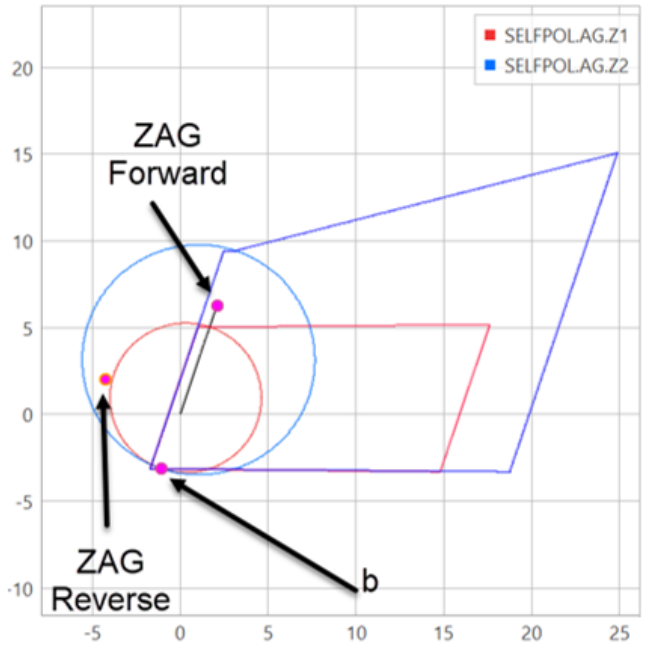

Fig. 10. Offset self-polarized distance element characteristics

The setting guidelines in Table I are applicable to the self-polarized mho and quadrilateral 21 elements.

TABLE I
OFFSET SELF-POLARIZED DISTANCE ELEMENT SETTINGS

		Zone 1	Zone 2
Mho and quad	Forward reach	0.8 • Z1MAG_MIN	1.5 • Z1MAG_MAX
	Reverse reach	–0.5 • Z1MAG_MIN	
Quad only	Tilt	$\arg\left[\frac{1}{1+k0_L}\right]-7$	$\arg\left[\frac{1}{1+k0_L}\right]+7$
	Left resistive reach	–0.1 • Z1MAG_MIN	
	Right resistive reach	3 • Z1G	2 • Z2G

The forward reach for Zone 1 is set to 80 percent of Z1MAG_MIN, which is the positive-sequence impedance to the first WTG. The forward reach for Zone 2 is set to 150 percent of Z1MAG_MAX, which is the positive-sequence

impedance of the entire collector feeder. The use of ground distance Zone 2 is appropriate if the WTGSU has high-speed unit protection (e.g., transformer differential) because a fixed Zone 2 time delay provides reliable coordination. If the WTGSU is protected with time-overcurrent protection, as is typical, then directional time-overcurrent elements are likely simpler to coordinate.

The Zone 1 and Zone 2 quadrilateral left resistive reach is set to a small value because we expect resistive faults to be along the right resistive axis. The Zone 1 quadrilateral right resistive reach is set conservatively considering potential transformer (PT) and current transformer (CT) errors [16] [17]. Equation (9) provides an R_{MAX} value that is in per-unit of the Zone 1 ground forward reach (Z1G) based on an assumed degree error (deg_{err}) in the voltage phasor angle. Using a reach of 0.8 per unit of Z1MAG_MIN and a deg_{err}=3, the Zone 1 resistive reach should not exceed a value of 4.78 • SIN (Z1ANG). An example secure resistive reach is three times the reactance reach.

$$R_{MAX} = \frac{1-m}{m} \bullet \frac{180}{\pi \bullet deg_{err}} \bullet \sin(Z1ANG) \tag{9}$$

The Zone 1 tilt should be set conservatively to prevent an overreach. Equation (10) provides guidance of how to set Zone 1 tilt for a self-polarized quad under a no-load condition by finding the angular difference between the total fault current (IF) and the relay contribution to the total fault current (IR).

$$T = \arg\left[\frac{1}{2 \bullet X_1 + X_0 \bullet (1+3 \bullet k0_L)}\right] = \arg\left[\frac{IF}{IR}\right]$$
$$\text{where:} \tag{10}$$
$$X_1 = \frac{ZR1 + (1-m) \bullet ZL1}{ZR1 + ZL1 + ZS1}, X_0 = \frac{ZR0 + (1-m) \bullet ZL0}{ZR0 + ZL0 + ZS0}$$

If we assume Z1R >> Z1S and Z0R >> Z0S, then (10) simplifies to (11). This simplification is within reason because a collector feeder with IBRs produces low fault current and acts as a weak source (large ZR1) compared to the source impedance behind the relaying point associated with the grid in parallel with multiple feeders (small ZS1).

$$T = \arg\left[\frac{1}{1+k0_L}\right] \tag{11}$$

We can also arrive at (11) by assuming a radial system and recognizing that the fault resistance for an AG fault has the faulted phase current (IA), not the faulted loop current (IAG) flowing through it. In a radial system with no load, IA = IG and the ground current (IAG) can be simplified, as shown in (12). Equation (12) shows that the apparent resistance has a different trajectory in the ZA plane (VA/IA) than the ZAG plane (VA/IAG). To account for this in the ZAG plane, we can tilt the reactance line based on (11).

$$\frac{VA}{IA} = Z1(1+k0_L) + R$$
$$\frac{VA}{IA(1+k0)} = \frac{VA}{IAG} = Z1 + \frac{R}{1+k0_L} \tag{12}$$

Load-flow direction also influences the apparent fault resistance in the ZAG plane. Reference [18] shows that during forward load-flow (load-out), the apparent resistance for a forward fault shifts down and to the right in the ZAG plane when compared to no load. For reverse load-flow (load-in), the apparent resistance shifts up and to the right instead. In a collector feeder application, we expect load-flow to be in the reverse direction (load-in) under normal conditions, meaning the apparent resistance is expected to shift up and to the right compared to no load. This behavior is beneficial for Zone 1 security as a Zone 1 overreach is less likely.

However, with IBRs on the collector feeder, traditional thinking can become troublesome. There is a possibility that the IBRs are absorbing power, rather than producing, during an LG fault. This makes the apparent impedance shift down and to the right during a resistive fault. This creates a potential security issue where Zone 1 can misoperate for faults outside the Zone 1 reach. However, when ZR1 >> ZS1, load-flow direction has little effect on Zone 1 performance.

To bias toward security, we set the Zone 1 tilt with a margin of –7 degrees. Zone 2 tilt is set with a dependability margin of +7 degrees. The reverse reach for both zones is set to –0.5 • Z1MAG_MIN. This allows sufficient dependability margin for close-in resistive faults.

B. Directional Ground Overcurrent Protection (51G/67G)

As noted in the introduction, a 21G element has better selectivity than a 67G element because it has fixed reach that is mostly independent of the source impedance. However, the 51G element might be simpler to coordinate with the protection at the WTGSU MV level, which is often a fuse. The 51G element can be set sensitively as the MV delta connection of the WTGSU prevents the 51G element from overreaching and operating for faults on the LV side of the WTGSU.

C. Protection Element Supervision and Dependability Enhancements

To provide adequate security for the sensitively set ground fault protection elements, the following supervisory functions are used:

- Voltage-based FIDS logic that allows ground fault protection to operate during an LG fault.
- Directional element tuned to the capacitive resistance-grounded MV circuit to restrain for reverse faults.
- Security timers for Zone 1.

To improve dependability for ground fault protection, the following functions are used:

- A zero-sequence overcurrent supervision that enables traditional ground protection when the NGR is bypassed.
- Delayed dropout and sequencing timers for ground distance Zone 2 and the electromechanical reset emulation for 51G to improve dependability for intermittent faults.

1) *Voltage-Based FIDS*

Because of the unpredictable nature of the 3I2 contribution of the IBRs during an LG fault, the appropriate ground loops are released based on the phase-to-ground voltage. The associated FIDS logic is shown in Fig. 11 for the AG loop. For an AG fault, the A-phase voltage collapses because of the NGR, whereas the B-phase and C-phase voltages typically rise. The voltage-based FIDS logic checks for an A-phase undervoltage and that the B-phase and C-phase voltages are healthy. The 27PG setting may be set to 0.6 pu of VG_{NOM} to allow FSA27 assertion for an intermittent or resistive AG fault. The 1.5 times multiplier is used to check for an overvoltage on the other phases to help ensure that FSA27 does not transiently assert for LLG faults. The word bit, fault-selection line-to-ground (FSLG), can provide the 67G and 51G elements additional security. When energizing the collector feeder and the transformers, CT saturation during inrush can challenge sensitive ground overcurrent elements [19]. The voltage-based FIDS logic adds security in this case because all energized phases have a voltage greater than 0.6 pu.

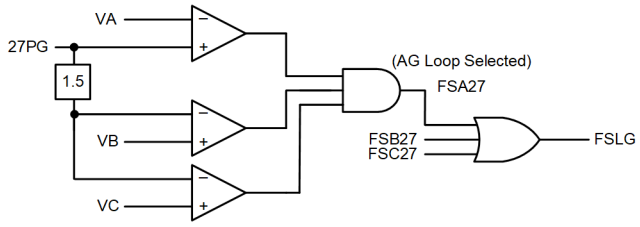

Fig. 11. Voltage-based FIDS logic for ground loop selection

2) *Directional Element for Resistance-Grounded Capacitive Systems*

Because the 3I2 overcurrent supervision for the 32Q element is set based on the collector feeder MVA rating, it may not be sensitive enough to use for LG fault detection. Therefore, we use the 32V element. However, as shown in Section II, using the collector cable zero-sequence impedance angle for the MTA setting of the 32V element can compromise security and dependability. To provide a secure and dependable directional element in a system in which the grounding resistor is sized closely to the capacitive reactance of the system, the MTA for the 32V element should be set at –45 degrees [4]. Fig. 12 shows the characteristic with the recommended MTA as well and the apparent zero-sequence impedance for a forward and reverse fault. With the MTA set at –45 degrees, the directional element declares forward for a source that is mainly resistive, mainly capacitive, or somewhere in between. The relay logic to implement the 32V element of Fig. 12 is included in Appendix D.

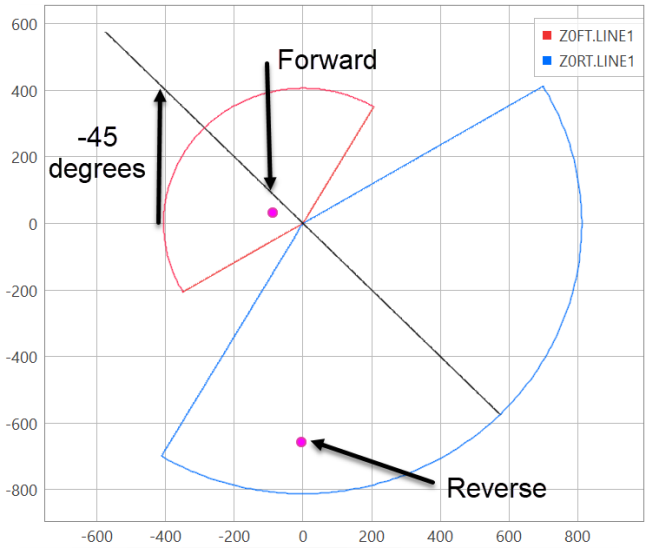

Fig. 12. Zero-sequence directional element for capacitive systems

3) *Zero-Sequence Current Supervision*

The 32V element works well when the NGR limits ground fault current. However, it is challenging for protection to detect a ground fault right at the transformer neutral that shorts the NGR [7] or a ground left due to maintenance. It is possible that an unintentional ground remains undiscovered until the first feeder ground fault occurs. To provide dependable collector feeder protection in such a scenario, the traditional 21G elements for effectively grounded systems may be enabled if 3I0 significantly exceeds (e.g., three times) the maximum NGR current (IG_{NGR}).

4) *21G Trip Logic Using Security and Dependability Timers*

Once the apparent impedance lies within the characteristics (ZAG in Zone Char.), the voltage-based FIDS logic is satisfied (FSA27), and the directional element indicates forward (32GF), Zone 1 can trip (21AG1T) after a short 0.5-cycle security timer. This is shown in Fig. 13. Zone 2 is typically configured with long time-delays, and it is possible for a loss of dependability during intermittent faults, which are common in these systems [7]. Using a sequencing timer adds dependability during intermittent faults. This timer accumulates toward a trip when 21AG2 asserts. If 21AG2 remains deasserted for six cycles, the sequencing timer resets its accumulated value and the overall Zone 2 timing logic is fully reset.

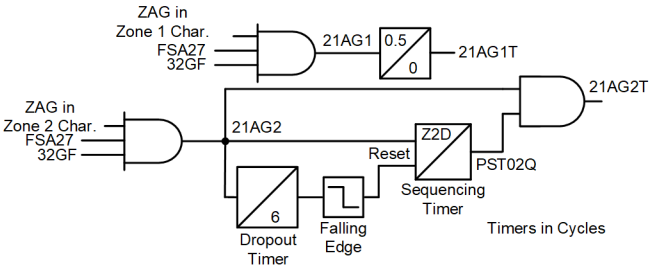

Fig. 13. Distance zone timer example

The performance of the logic of Fig. 13 is shown using a field event of an intermittent ground fault on a 13.8 kV system [7]. The event corresponds to a ground fault on the transformer bushing, and we manipulated the currents and voltages to move the fault to the other side of the CTs so it corresponds to a forward fault. The event is shown in Fig. 14 The directional element declares forward, the B-phase is selected, and 21AG1T trips.

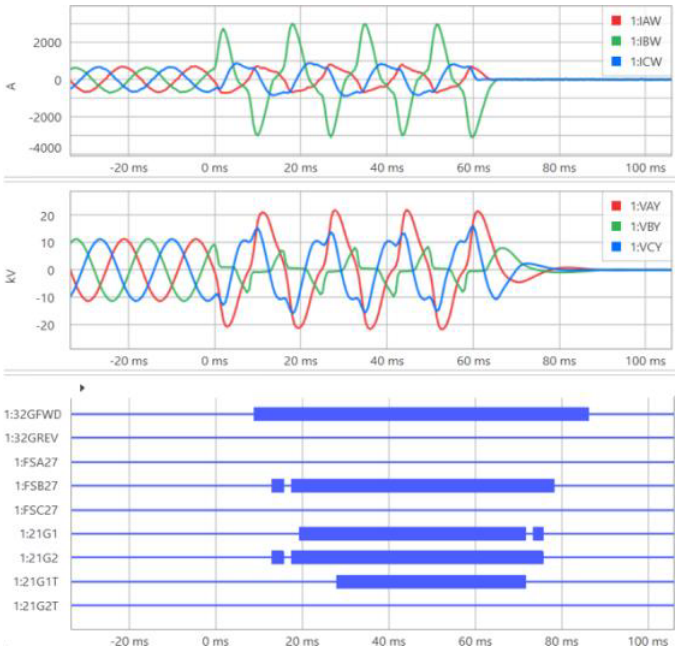

Fig. 14. Zone 1 operates for an intermittent ground fault field event

An intermittent ground fault is placed on Zone 2 of a 34.5 kV simulated system using the intermittent logic shown in Fig. 13 from [20]. The result of implementing this logic is shown in Fig. 15. The Zone 2 time delay is set to nine cycles and the dropout timer delay is shortened to three cycles to better illustrate the event. The sequencing timer continues to accumulate despite intermittent dropouts, and 21AG2T remains dependable.

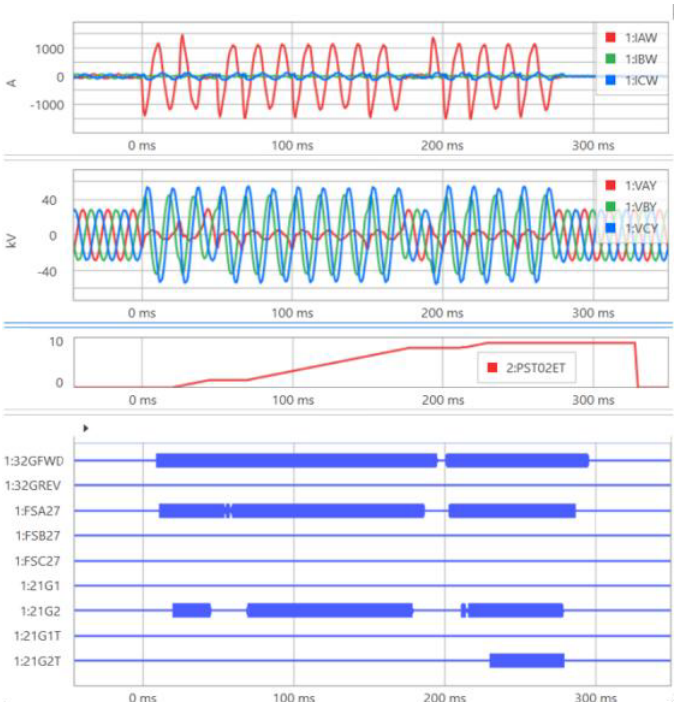

Fig. 15. Zone 2 operates for a simulated intermittent ground fault

5) *67G Trip Logic Using Security and Dependability Timers*

The logic in Fig. 13 was revised to show implementation for the 67G element set as the underreaching Zone 1 and a 51G element set as the overreaching Zone 2. See Fig. 16 for the revised logic.

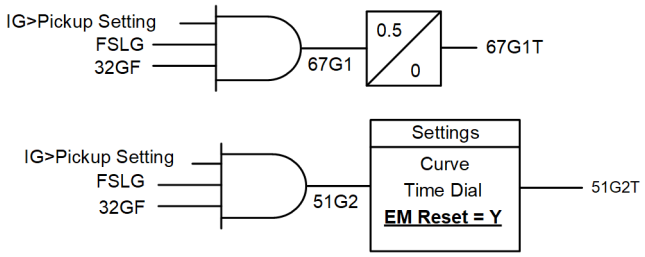

Fig. 16. Zone 1 67G timer and Zone 2 51G example

The 51G2T takes advantage of the electromechanical reset emulation to provide dependability for intermittent arcing faults. Both elements use the directional element for resistance-grounded capacitive systems and the voltage-based FIDS logic for security.

V. Conclusion

Medium-voltage collector systems with a neutral grounding resistor and significant cable capacitances challenge traditional directional and distance protection. In this paper, we discuss the challenges in these systems when inverter-based resources are connected to the collector feeders. The challenges include:

- Memory-polarized distance elements may lose dependability for forward faults (Fig. 3) and security for reverse faults (Fig. 7).
- Zero-sequence directional elements set with the protected cable's inductive zero-sequence impedance angle for the MTA setting have reduced dependability (Fig. 6) and security (Fig. 9).
- Intermittent arcing faults can reduce dependability of time-delayed protection elements.
- Current-based FIDS logic and the negative-sequence directional element can be unreliable near IBRs [2].

The solutions to these challenges are:

- Use fault-loop polarized distance elements to prevent dynamic performance misbehavior associated with memory polarization (Fig. 10).
- Use voltage-based FIDS logic (Fig. 11) and set protection that uses 3I2 based on the maximum expected collector feeder ratings.
- Set the zero-sequence directional element's MTA based on the parallel combination of the NGR and the cable capacitances. A reasonable value is –45 degrees (Fig. 12).
- Use conditional and sequencing timers to improve security for Zone 1 transients and Zone 2 dependability for intermittent arcing faults (Fig. 13) and Fig. 16).

The solutions can be implemented in distance relays using the programmable logic shown in the Appendix and [15].

VI. Appendix

A. Apparent Source Impedance for Mismatch Based on k0S and k0L(Forward Fault)

The apparent source impedance for a forward A-phase to ground fault are given in (13). From these, the *b* point of the mho circle is defined.

$$-\left[\frac{V1_{mem}-VA}{IA+K0_L \bullet IG}\right]\bullet\left[\frac{IA+k0_L \bullet IG}{IA+k0_s \bullet IG}\right]=-ZS1$$

$$-\left[\frac{V1_{mem}-VA}{IA+K0_L \bullet IG}\right]=-ZS1\bullet\left[\frac{IA+k0_S \bullet IG}{IA+k0_L \bullet IG}\right]=b_{V1MEM} \quad (13)$$

If we assume that IA=IG, we can further simplify as shown in (14).

$$-\left[\frac{V1_{mem}-VA}{IA+K0_L \bullet IG}\right]=-ZS1\bullet\left[\frac{1+k0_S}{1+k0_L}\right]=b_{V1MEM} \quad (14)$$

In Fig. 2, we can see that XC0 of the faulted feeder provides infeed to the fault and the relay will not see IA=IG. As such (13) provides more accurate results, while (14) offers a simplified approximation.

Equation (14) provides the approximate *b* point when positive-sequence memory voltage is used for polarization. When memory expires, the *b* point will be a function of the positive-sequence voltage, not the positive-sequence memory voltage. This point is given in (15) from [11].

$$-ZS1\bullet\left[\frac{\frac{2}{3}+k0_S}{1+k0_L}\right]=b_{V1} \quad (15)$$

Because k0s is very large in the systems described in this paper, (14) and (15) are nearly the same.

B. Find Position of the Quadrilateral Characteristic Directional Line in the Apparent Impedance Plane

The technique to find the location of quadrilateral directional lines in the apparent impedance plane is detailed in [11].

The directional line can be represented as an impedance line with a reach set at 0 ohms.

$$SOP = V1_{MEM} - IAG \bullet 0$$
$$SPOL = IAG \bullet (1\angle Z1ANG)$$

From this we can divide SOP by IAG to find the apparent reach of the line.

$$\frac{SOP}{IAG}=\frac{V1_{mem}}{IAG}$$
$$\frac{SOP}{IAG}=\frac{V1_{mem}}{IAG}+\frac{VA}{IAG}-\frac{VA}{IAG}$$
$$\frac{SOP}{IAG}=\frac{VA}{IAG}-\left(\frac{-V1_{mem}+VA}{IAG}\right)$$
$$\frac{SOP}{IAG}=ZAG-\left(-ZS1_{APP}\right)$$

The forward reach is –ZS1APP.

We introduce the term VA/∞ to account for the absence of voltage in the polarizing signal.

$$SPOL=\frac{VA}{\infty}+IAG\bullet(1\angle Z1ANG)$$

We divide SPOL by IAG to find the *b* point.

$$\frac{SPOL}{IAG}=\frac{VA}{\infty \bullet IAG}+\frac{IAG\bullet(1\angle Z1ANG)}{IAG}$$
$$\frac{SPOL}{IAG}=\frac{1}{\infty}\left[\frac{VA}{IAG}+\left(\infty\angle Z1ANG\right)\right]$$
$$\frac{SPOL}{IAG}=\frac{1}{\infty}\left[ZAG+\left(\infty\angle Z1ANG\right)\right]$$

The reverse reach is (–) ∞ at an angle of Z1ANG.

The directional line slides along Z1ANG with reach of –ZS1.

C. Apparent Remote Source Impedance (Reverse Fault)

For a reverse fault with the IBR breakers open, IAG is pure zero-sequence (neglecting any positive-sequence capacitance line charging current present). This allows us to simplify IAG for reverse faults.

$$IAG = I0 + k0 \bullet 3I0$$

$$IAG = I0 + \frac{Z0 - Z1}{3 * Z1} \bullet 3I0$$

$$IAG = I0 \frac{Z0_L}{Z1_L}$$

$$\left[\frac{V1_{mem} - VA}{I0 \frac{Z0_L}{Z1_L}} \right] \bullet \left[\frac{I0 \frac{Z0_L}{Z1_L}}{I0 \frac{Z0_R}{Z1_R}} \right] = -ZR1$$

$$\left[\frac{V1_{mem} - VA}{I0 \frac{Z0_L}{Z1_L}} \right] \bullet \left[\frac{Z0_L \bullet Z1_R}{Z1_L \bullet Z0_R} \right] = -ZR1$$

$$\left[\frac{V1_{mem} - VA}{I0 \frac{Z0_L}{Z1_L}} \right] = -ZR1 \bullet \left[\frac{Z1_L \bullet Z0_R}{Z0_L \bullet Z1_R} \right]$$

$$\left[\frac{V1_{mem} - VA}{I0 \frac{Z0_L}{Z1_L}} \right] = -Z0_R \bullet \left[\frac{Z1_L}{Z0_L} \right] = b_{reverse}$$

D. Zero-Sequence Directional Element Logic

The logic provided below implements a zero-sequence impedance directional element, as detailed in [12]. This logic allows a user to set a favorable MTA for the systems discussed in this paper.

```
1: ### SETTINGS
2: PMV64:= –45.000000 #SETTING Z0ANG
3: PMV63:= 0.500000 #50GFP
4: PMV62:= 0.250000 #50GRP
5: PMV61:= 0.100000 # A0 FACTOR
6: ###
7: PMV60:= 3V0FIM * LIGFIM * COS(3V0FIA – LIGFIA – PMV64)/(LIGFIM * LIGFIM) #Z0
8: PMV59:= 0.750000 * –0.300000 – 0.250000 * (3V0FIM/LIGFIM) #Z0FTH
9: PMV58:= –PMV59 #Z0RTH
10: PMV57:= PMV61 * LI1FIM * 3.000000 # A0 * 3I1
11: PSV64:= NOT (SPO OR ILOP) AND LIGFIM > PMV57 AND (LIGFIM > PMV62 OR LIGFIM > PMV63) #32VE
12: PCT32IN:= PMV60 < PMV59 AND LIGFIM > PMV63 AND PSV64 # FORWARD AND 50GF AND 32VE
13: PCT32PU:= 0.500000
14: PCT31IN:= PMV60 > PMV58 AND LIGFIM > PMV62 AND PSV64 #REVERSE AND 50GR AND 32VE
15: PCT31PU:= 0.500000
16: #F32V = PCT32Q
17: #R32V = PCT31Q
```

VII. References

[1] E. O. Schweitzer and J. Roberts, "Distance Relay Element Design," proceedings of the 19th Annual Western Protective Relay Conference, Spokane, WA, October 1992.

[2] R. Chowdhury and N. Fischer, "Transmission Line Protection for System With Inverter-Based Resources – Part I: Problems," in IEEE Transactions on Power Delivery, vol. 36, no. 4, pp. 2416–2425, Aug. 2021, doi: 10.1109/TPWRD.2020.3019990.

[3] R. Chowdhury and N. Fischer, "Transmission Line Protection for System With Inverter-Based Resources – Part II: Solutions," in IEEE Transactions on Power Delivery, vol. 36, no. 4, pp. 2426–2433, Aug. 2021, doi: 10.1109/TPWRD.2020.3030168.

[4] R. Lavorin, D. Hou, H. J. Altuve, N. Fischer, and F. Calero, "Selecting Directional Elements for Impedance-Grounded Distribution Systems," proceedings of the 34th Annual Western Protective Rely Conference, Spokane, WA, October 2007.

[5] A. Tsylin, R. Kruse-Nielsen, G. Yang and B. Sedaghat, "Influence of collection network parameters on performance of distance protection directional elements in offshore wind farms," 15th International Conference on Developments in Power System Protection (DPSP 2020), 2020, pp. 1–6, doi: 10.1049/cp.2020.0113.

[6] IEEE Std 2800, *IEEE Standard for Interconnection and Interoperability of Inverter-Based Resources (IBRs) Interconnecting with Associated Transmission Electric Power Systems*.

[7] R. Chowdhury, M Alla, N. Fischer, and S. Samineni, "Restricted Earth Fault Protection in Low-Impedance Grounded System With Inverter-Based Resources," in IEEE Transactions on Power Delivery, 2022, doi: 10.1109/TPWRD.2022.3195741.

[8] IEEE Std C62.92.1-2016, *IEEE Guide for the Application of Neutral Grounding in Electrical Utility Systems—Part I: Introduction*.

[9] D. D. Fentie, "Understanding the dynamic mho distance characteristic," 2016 69th Annual Conference for Protective Relay Engineers (CPRE), 2016, pp. 1–15, doi: 10.1109/CPRE.2016.7914922.

[10] D. Tziouvaras, "Protection of High-Voltage AC Cables," 59th Annual Conference for Protective Relay Engineers, 2006., 2006, pp. 48–61, doi: 10.1109/CPRE.2006.1638691.

[11] F. Calero, "Distance elements: Linking theory with testing," 2009 62nd Annual Conference for Protective Relay Engineers, 2009, pp. 333–352, doi: 10.1109/CPRE.2009.4982524.

[12] J. Roberts and A. Guzmán, "Directional Element Design and Evaluation" proceedings of the 21st Annual Western Protective Relay Conference, Spokane, WA, October 1994.

[13] R. McDaniel and M. J. Thompson, "Impedance-Based directional Element – Why Have a Threshold Setting?" proceedings of the 48th Annual Western Protective Relay Conference, October 2021.

[14] B. Kasztenny, "Distance Elements for Line Protection Applications Near Unconventional Sources," proceedings of the 75th Annual Conference for Protective Relay Engineers, March 2021.

[15] R. McDaniel and Y. Shah, "Programming Non-Directional Distance Elements in the SEL-411L-1 and SEL-421-5," SEL Application Guide Available December 2022.

[16] G. Alexander, "Guidelines for Setting Quadrilateral Ground Distance Elements," SEL Application Guide (AG2015-14), 2015. Available: selinc.com.

[17] J. Mooney and J. Peer, "Application Guidelines for Ground Fault Protection," proceedings of the 24th Annual Western Protective Relay Conference, October 1997.

[18] B. Kasztenny, "Setting Considerations for Distance Elements in Line Protection Applications," proceedings of the 74th Annual Conference for Protective Relay Engineers, March 2021.

[19] R. Chowdhury, N. Fischer, D. Taylor, D. Caverly, and A. B. Dehkordi, "A Fresh Look at Practical Shunt Reactor Protection," proceedings of the 49th Annual Western Protective Relay Conference, Spokane, WA, October 2022.

[20] A. B. Dehkordi, R. Chowdhury, N. Fischer, and D. Finney, "Generator Protection Validation Testing Using a Real-Time Digital Simulator: Stator Winding Protection," proceedings of the 48th Annual Western Protective Relay Conference, October 2021.

VIII. Biographies

Ryan McDaniel earned his BS in computer engineering from Ohio Northern University in 2002. In 1999, he was hired by American Electric Power (AEP) where he worked as a relay technician and a protection and control engineer. In 2005, he joined Schweitzer Engineering Laboratories, Inc. and is currently a Principal engineer. His responsibilities include providing application support and technical training for protective relay users. Ryan is a registered professional engineer in the state of Illinois and a member of the IEEE

Ritwik Chowdhury received his BS degree in engineering from the University of British Columbia and his MS degree in engineering from the University of Toronto. He joined Schweitzer Engineering Laboratories, Inc. (SEL) in 2012, where he is presently a senior engineer in research and development. Ritwik holds 9 patents and has helped author 25 technical papers. He was recognized as an exceptional reviewer for IEEE Transactions on Power Delivery for 2019 and 2021. He is the vice chair of the Protection and Control Practices Subcommittee (I-SC) of the IEEE PSRC Committee, the chair of two IEEE Standards Working Groups, and the recipient of the 2021 PSRC Outstanding Young Engineer Award. Ritwik is a senior member of the IEEE and a registered professional engineer in the province of Ontario.